A MODEL FOR DUST PARTICLES ORBITING THE NUCLEI OF COMETS. P. Tricarico[1] and N. Samarasinha[2], [1,2]*Planetary Science Institute, 1700 E. Ft. Lowell # 106, Tucson AZ 85719, USA,* [1]*tricaric@psi.edu,* [2]*nalin@psi.edu*.

Motivation. The existence of bound dust particles around cometary nuclei has been argued based on analytical grounds [e.g., 1-2], and demonstrated numerically [3-5]. Dust particles emitted by cometary nuclei could stay in temporary bound orbits around the nuclei for timescales as large as weeks or months or even longer. These particles could act as a reservoir of cometary dust and may explain some of the baffling observations that have so far eluded a self-consistent interpretation.

In the case of comet 1P/Halley, the gas production rates (and in particular of the H_2O photo-dissociation product OH) are nearly symmetric pre- and post-perihelion. On the other hand, the dust production rate is consistently higher in the post-perihelion by approximately factor three [6]. For a comet that is in a principal axis rotation, this could be due to seasonal effects. However, for comet 1P/Halley, which is in a non-principal axis spin state [7,8], it was shown by [9] that the subsolar point traverses the entire nucleus over "diurnal" timescales and no seasonal effects are likely.

In this abstract, we show that based on our preliminary work, it is indeed possible to have higher dust-to-gas ratios during the post-perihelion leg due to dust particles in temporary bound orbits.

Model. The temporary bound trajectories of particles primarily lie within the bound coma radius $R_{\rm bound}$ defined as:

$$R_{\rm bound} = \min\{R_{\rm exo}, R_{\rm Hill}\} \quad (1)$$

$$R_{\rm Hill} = r_{\rm h}\left(\frac{M_N}{3M_\odot}\right)^{1/3} \quad (2)$$

$$R_{\rm exo} = r_{\rm h}\left(\frac{M_N}{\beta M_\odot}\right)^{1/2} \quad (3)$$

where $R_{\rm Hill}$ is the Hill-sphere radius determined by the stable region for a satellite under the mutual gravity of the comet and the Sun, $R_{\rm exo}$ is the exopause radius defined to be the distance at which the gravitational attraction of the comet equals the radiation pressure force [10], $r_{\rm h}$ is the heliocentric distance, M_N is the mass of the comet nucleus, $M_\odot$ is the solar mass, β is the ratio between the forces due to solar radiation pressure and the gravity of the Sun [11].

In Figure 1 we show $R_{\rm bound}$ as a function of the comet nucleus radius and dust particle radius for a comet at a heliocentric distance of 1 AU. A comet bulk density of 0.5 g cm^{-3} and a particle bulk density of 1.0 g cm^{-3} are assumed. Since $R_{\rm bound}$ scales linearly with $r_{\rm h}$, its value for different $r_{\rm h}$ can be calculated easily. The curves of constant $R_{\rm bound}$ are shown by dashed lines. The bold line marks the boundary between the region where $R_{\rm Hill} < R_{\rm exo}$ (above the line) and the region where $R_{\rm exo} < R_{\rm Hill}$ (below the line). The grey area on

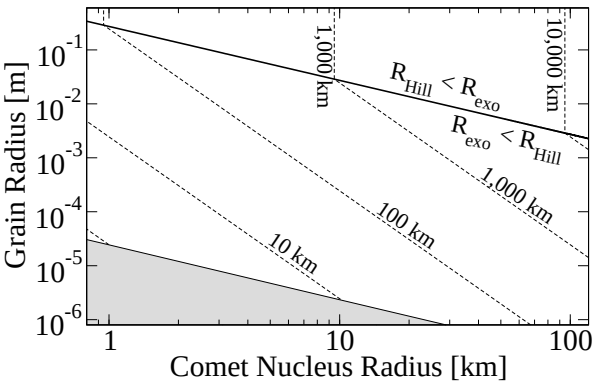

Figure 1: Value of $R_{\rm bound} = \min\{R_{\rm exo}, R_{\rm Hill}\}$ as a function of comet nucleus radius and particle radius, at $r_{\rm h} = 1$ AU.

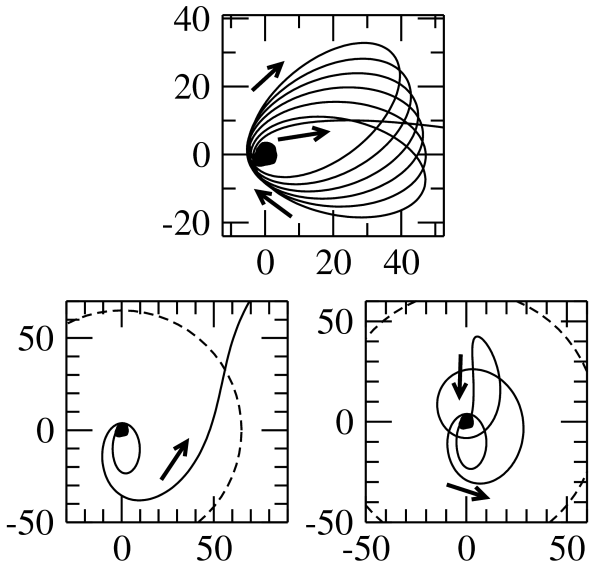

Figure 2: Numerical modeling of the trajectories of dust particles ejected from the nucleus. Top: trajectory of a particle ($\beta = 10^{-5}$, particle radius $r_{\rm g} \simeq 6$ cm) ejected at a velocity $0.97 \times V_{\rm esc}$ when $R_{\rm bound} \simeq 250$ km. Bottom: trajectory of two slightly different particles ($\beta = 1.45 \times 10^{-4}$ in left figure, $\beta = 1.50 \times 10^{-4}$ in right figure, $r_{\rm g} \simeq 4$ mm in both cases) ejected at a velocity $0.95 \times V_{\rm esc}$ when $R_{\rm bound} \simeq 65$ km. The dashed curves mark the value of $R_{\rm bound}$. Scale is in km.

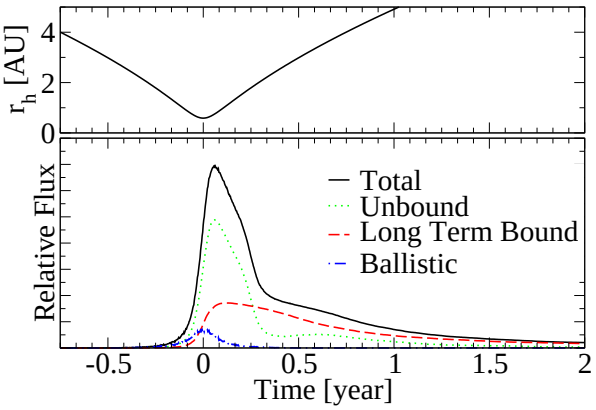

Figure 3: Heliocentric distance $r_{\rm h}$ (top) and modeled flux (bottom) due to dust particles for comet 1P/Halley. Zero time is at the perihelion. Small tick marks represent months. The total flux (black continuous line) is the sum of the contributes from escaping particles (green dotted line), bound particles (red dashed line), and ballistic particles (blue dot-dash line).

the bottom marks where $R_{\rm bound}$ is less than or equal to the radius of the comet nucleus. If a comet has a nucleus radius of $\simeq$ 10 km, for $R_{\rm bound} = R_{\rm Hill} \simeq$ 1,000 km, a particle of radius $\geq$ 3 cm can remain bound anywhere within 1,000 km from the nucleus. On the other hand, a particle of radius 300 μm must be within 100 km from the nucleus to be bound.

Whether a particle will escape the nucleus gravity or will be in a bound trajectory depends on the net ejection velocity, $V_{\rm eje}$, of the dust particle from the nucleus. Broadly speaking, if $V_{\rm eje}$ is between $V_{\rm esc}$ and $V_{\rm esc}/\sqrt{2}$, then the particle can be propelled into a bound orbit [12]. Here $V_{\rm esc}$ is the escape velocity of the comet and $V_{\rm esc}/\sqrt{2}$ corresponds to the orbital velocity of a circular orbit having a radius equal to that of the nucleus. However, in reality, the orbits of the ejected particles are highly elongated and only a small range of net ejection velocities just below the escape velocity are capable of putting a particle into a bound orbit. For nuclei of a few km radius representative of most comets, the escape velocity is of the order of one meter per second. At $r_{\rm h} = 1$ AU, ejection velocities are of the order of one meter per second for few cm-sized particles which in turn are comparable to escape velocities of few km radius nuclei.

Initial Results. The first step consists of integrating the dynamics of a particle ejected from the surface of a comet nucleus under the influence of the gravity of the non-spherical rotating nucleus, which could be either a non-principal axis rotator or a principal axis rotator. It also includes solar gravity and the radiation pressure. Currently, the gas drag and dust fragmentation are not modeled, but will be included soon. Examples of the resulting near-nucleus dynamics are shown in Figure 2, where three classes of evolution are displayed: particles escaping after being in a bound orbit (top), particles escaping shortly after ejection from the nucleus (bottom left), and particles which fall back on to the comet after being in a bound orbit (bottom right).

To simulate a large number of particles, and obtain measurable quantities out of these preliminary simulations, we follow a statistical approach, where the details of the dynamics of each particle are synthesized to determine the probability to stay in a bound orbit, fall back on to the nucleus surface, or escape the comet. The probability of each dynamical outcome is very sensitive to the radiation pressure (β) and initial conditions (ejection velocity, location of ejection) of the particle, as well as the mass, shape, rotational state, and the orbit of the nucleus. Once all these probabilities corresponding to the relevant parameters have been determined for a given comet, it is possible to model measurable quantities such as the flux in continuum bands and compare the model with data.

One example of our preliminary modeling is shown in Figure 3 where the flux due to dust particles is plotted for comet 1P/Halley during a perihelion passage. The two classes of the flux in the figure are escaping particles and bound particles. The first class represents particles that escape the gravity of the nucleus, while the second class represents particles that stay in orbit around the nucleus for a long period. The latter will ultimately fall back on to the nucleus or escape. When bound particles are perturbed into an escaping trajectory, their flux contribution goes into the escaping particles class.

Discussion. As we show in Figure 3, it is possible to explain the observed pre- and post-perihelion asymmetry in the dust, while maintaining a symmetric production rate. This model, with the addition of the necessary modifications, has the potential to investigate the icy grains observed by the EPOXI spacecraft around comet 103P/Hartley 2.

Acknowledgments. This work is supported by the NASA Planetary Atmospheres Program.

References. [1] Meech K. J. and Belton M. J. S. (1990) *AJ, 100*, 1323. [2] Richter K. and Keller H. U. (1995) *Icarus, 114*, 355. [3] Fulle M. (1997) *A&A, 325*, 1237. [4] Scheeres D. J. and Marzari F. (2000) *A&A, 356*, 747. [5] Mach K. D. and Samarasinha N. H. (2000) *BAAS, 32*, 1032. [6] Schleicher D. G. et al. (1998.) *Icarus, 132*, 397. [7] Belton, M. J. S. et al. (1991) *Icarus, 93*, 183. [8] Samarasinha N. H. and A'Hearn M. F. (1991.) *Icarus, 93*, 194. [9] Rickman H. (1989) *Adv. Sp. Res., 9*, 59. [10] Bishop J. (1985) *JGR, 90*, 5235. [11] Burns J. A. et al. (1979) *Icarus, 40*, 1. [12] Stern S. A. et al. (1994) *AJ, 107*, 765.